

# Multifunctional Layer-by-Layer Coating of Digitally Encoded Microparticles

Stefaan Derveaux,<sup>†</sup> Bruno G. De Geest,<sup>†</sup> Chris Roelant,<sup>‡</sup> Kevin Braeckmans,<sup>†</sup>  
Jo Demeester,<sup>†</sup> and Stefaan C. De Smedt<sup>\*,†</sup>

Laboratory of General Biochemistry and Physical Pharmacy, University of Ghent, Harelbekestraat 72,  
9000 Ghent, and Memobead Technologies NV, Rupelweg 10, 2850 Boom, Belgium

Received March 5, 2007. In Final Form: June 25, 2007

In the field of medical diagnostics there is a growing need for inexpensive, accurate, and quick “multiplexing” assays. By making use of encoded microparticles, such assays allow simultaneous determination of the presence of several analytes in a biological sample. The microparticles under investigation in this study are encoded by writing a digital dot or bar code in their central plane. This study evaluates to what extent a “multifunctional” coating can be applied around the digitally encoded microparticles by the layer-by-layer (LbL) technology. We show that a LbL coating containing CrO<sub>2</sub> nanoparticles allows (a) an optimal (optical) readout of the dot and bar codes, (b) a perfect orientation of the microparticles, necessary to be able to read the code, and (c) an optimal coupling of capture probes to the surface of the microparticles.

## Introduction

Driven by the human genome project, an increasing number of genes related to diseases have been discovered. As a result, tools are needed to carry out inexpensive, accurate, and quick genetic diagnostic analyses. In recent years, “multiplexing” diagnostic assays have been developed. While a “monoplex” assay aims to measure the binding of a single analyte in the biological sample to its receptor, a multiplexing assay aims to measure *simultaneously* the binding of several analytes in the biological sample to their respective receptors.<sup>1</sup>

Multiplex technologies are divided into two categories, “flat surface arrays” and “suspension arrays”.<sup>2</sup> To the first category belong the well-known DNA microarrays, using the x,y-coordinates of spots of single-stranded DNA (called probes) on a glass plate to identify which DNA targets are present in a sample.<sup>3</sup> Despite the success of DNA microarrays, they lack efficient reactions between the probes and the targets due to, among other reasons, slow diffusion of the target DNA molecules toward the probes on the flat surface.<sup>4</sup> Furthermore, flat microarray technology copes with localization problems upon miniaturization, while its use has also been limited by the high cost of the microarray consumables and the instruments. Suspension arrays have a number of advantages compared to flat microarrays, regarding for instance the attachment of probes, the flexibility in composing a test panel, and improved kinetics.<sup>5–8</sup> The second category, suspension arrays, uses *encoded* micrometer-sized particles for multiplexing; the code identifies which probe is

bound to the surface of the microparticles. Targets present in the biological sample will bind to their corresponding microparticles that are added to the sample. By decoding the microparticles that show a positive reaction, the target molecules that are present in the sample can be identified.

Various strategies have been applied to encode microparticles: spectrometric,<sup>6</sup> electronic,<sup>6</sup> physical,<sup>9–11</sup> and graphical<sup>12,13</sup> encoding. Each of the encoding technologies has its strengths and weaknesses, as reviewed by Braeckmans et al.<sup>14</sup> Our group has reported “spatial selective photobleaching” as a new method to digitally encode fluorescent microspheres.<sup>15</sup> As parts A and B of Figure 1 show, digital codes (such as a bar code, a dot code, ...) can be written in the *central plane* of fluorescent polystyrene microspheres (called memobeads) by localized photobleaching of the fluorescent molecules. Clearly, as microspheres are free to rotate in the assay tube, to be able to read the digital code (at the end of the assay), the microspheres must be properly oriented with respect to the focal plane of the microscope (Figure 1C). For this purpose we have suggested loading the microspheres with ferromagnetic particles (e.g., CrO<sub>2</sub>).<sup>15</sup> Ferromagnetic materials become magnetized in an external magnetic field and remain magnetized for a period after the material is no longer in the field (a net magnetic moment is present in the absence of the external magnetic field, called remanence, or “magnetic memory”). The encoding process of the microspheres in this study consists of two steps, a writing step (i.e., the photobleaching process) and a magnetizing step, during which the CrO<sub>2</sub>-loaded microspheres are exposed to an external magnetic field sufficient to provide them with a magnetic memory. The microspheres are

- \* To whom correspondence should be addressed. Phone: 00 32 9 264 8076. Fax: 00 32 9 264 81 89. E-mail: stefaan.desmedt@ugent.be.
- <sup>†</sup> University of Ghent.
- <sup>‡</sup> Memobead Technologies NV.
- (1) Ling, M. M.; Ricks, C.; Lea, P. *Expert Rev. Mol. Diagn.* **2007**, 7 (1), 87–98.
- (2) Venkatasubbarao, S. *Trends Biotechnol.* **2004**, 22 (12), 630–637.
- (3) Southern, E. M. *Methods Mol. Biol.* **2001**, 170, 1–15.
- (4) Vainrub, A.; Pettitt, B. M. *Phys. Rev. E: Stat., Nonlinear, Soft Matter Phys.* **2002**, 66 (4, Part 1), 041905.
- (5) Henry, M. R.; Wilkins, S. P.; Sun, J.; Kelso, D. M. *Anal. Biochem.* **1999**, 276 (2), 204–214.
- (6) Czarnik, A. W. *Curr. Opin. Chem. Biol.* **1997**, 1 (1), 60–66.
- (7) Wilson, R.; Cossins, A. R.; Spiller, D. G. *Angew. Chem., Int. Ed* **2006**, 45 (37), 6104–6117.
- (8) Nolan, J. P.; Sklar, L. A. *Trends Biotechnol.* **2002**, 20 (1), 9–12.

(9) McHugh, T. M.; Miner, R. C.; Logan, L. H.; Stites, D. P. *J. Clin. Microbiol.* **1988**, 26 (10), 1957–1961.

(10) Scilliani, J. J.; McHugh, T. M.; Busch, M. P.; Tam, M.; Fulwyler, M. J.; Chien, D. Y.; Vyas, G. N. *Blood* **1989**, 73 (7), 2041–2048.

(11) Martens, C.; Bakker, A.; Rodriguez, A.; Mortensen, R. B.; Barrett, R. W. *Anal. Biochem.* **1999**, 273 (1), 20–31.

(12) Pantano, P.; Meek, C. C.; Wang, J.; Coutinho, D. H.; Balkus Jr, K. J. *Lab Chip* **2003**, 3 (2), 132–135.

(13) Nicewarner-Pena, S. R.; Freeman, R. G.; Reiss, B. D.; He, L.; Pena, D. J.; Walton, I. D.; Cromer, R.; Keating, C. D.; Nolan, M. J. *Science* **2001**, 294 (5540), 137–141.

(14) Braeckmans, K.; De Smedt, S. C.; Leblans, M.; Pauwels, R.; Demeester, J. *Nat. Rev. Drug Discovery* **2002**, 1 (6), 447–456.

(15) Braeckmans, K.; De Smedt, S. C.; Roelant, C.; Leblans, M.; Pauwels, R.; Demeester, J. *Nat. Mater.* **2003**, 2 (3), 169–173.

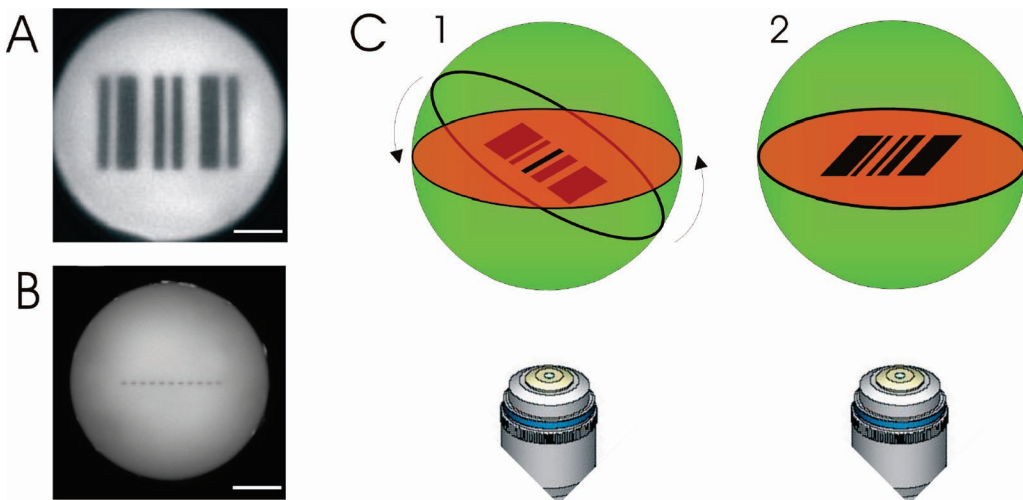


**Figure 1.** Confocal images of the central plane of nonmagnetic fluorescent microspheres encoded with a bar code (A) and a dot code (B). The scale bar is 10  $\mu\text{m}$ . (C) The encoded microsphere has to be properly oriented at the time of decoding to be able to read the entire code. At position 1, the code is tilted with respect to the microscope focal plane and only the intersection of the code with the focal plane is visible. At position 2, the entire code is visible because it coincides with the focal plane.

fixed on a grid during the encoding process to avoid rotation between the two steps. At the decoding step, the ferromagnetic microspheres are again exposed to a (weak) magnetic field with the same orientation as the first one (relative to the direction of the laser light). In the presence of this weak magnetic field, the “remanent” nanoparticles tend to align with the magnetic field, so they will turn the microspheres at the surface to which they are fixed. The magnetic forces enable the orientation of the microspheres into such a position that the code can be read (the code is present in a plane perpendicular to the direction of the laser light).<sup>15</sup> A software program can detect the orientation of the code within that plane, so that one magnetic field component is enough for the orientation of the microspheres.

Various methods have been developed for the production of magnetic microspheres. They include the deposition of nanoparticles in polymer particles by dispersion copolymerization of polymers in the presence of magnetic nanoparticles<sup>16</sup> or by “activated swelling”.<sup>17</sup> Some groups reported the use of block copolymer systems for the controlled formation of a homogeneous nanoparticle pattern on a planar surface;<sup>18,19</sup> the pattern formation of nanoparticles on flat surfaces seemed to be perfectly tunable via this approach.<sup>20</sup> Bhat et al. reported another interesting method to fine-tune the number density of nanoparticles on a planar substrate by tailoring of attachment points on that substrate.<sup>21</sup> To our knowledge neither of these last two approaches has been applied to microspheres. Skirtach et al. could control the distribution of nanoparticles within polyelectrolyte capsules by polymers.<sup>22</sup>

With the aim of properly orienting digitally encoded microspheres, we examine in this paper whether memobeads can be coated with sub 500 nm CrO<sub>2</sub> nanoparticles by layer-by-layer (LbL) technology, which is based on the alternate adsorption of

oppositely charged polyelectrolytes/nanoparticles onto a charged substrate.<sup>23–25</sup> The major aims are to evaluate whether the magnetic LbL coating is indeed multifunctional in the sense that the LbL coating (a) allows positioning of the memobeads for decoding, (b) does not optically interfere with the encoding and reading process, and (c) allows a high and homogeneous loading of the surface of the microspheres with probes.

## Experimental Section

**Materials.** Nonmagnetic and ferromagnetic green fluorescent carboxylated polystyrene microspheres (39  $\mu\text{m}$  in diameter) were purchased from Spherotech (Libertyville, IL).

Poly(allylamine hydrochloride) (PAH; MW  $\approx$  70 000), sodium poly(styrenesulfonate) (PSS; MW  $\approx$  70 000), and poly(acrylic acid) (PAA; MW  $\approx$  450 000) were obtained from Sigma-Aldrich (Steinheim, Germany). A 5'-Cy5-terminal 3'-amino-terminal labeled 29-mer oligonucleotide was purchased from Eurogentec (Seraing, Belgium). Bovine serum albumine (BSA) and 2-(N-morpholino)-ethanesulfonic acid (MES) were purchased from Sigma, Dulbecco's PBS was purchased from Invitrogen (Merelbeke, Belgium), and Tween-20 was purchased from Calbiochem (Darmstadt, Germany). EDC (1-ethyl-3-[3-(dimethylamino)propyl]carbodiimide hydrochloride) was obtained from Perbio Science (Erembodegem, Belgium).

**Layer-by-Layer Coating of the Microspheres.** PAH and PSS stock solutions were prepared in 0.5M NaCl (2 mg/mL). PAA was dissolved in 0.5M NaCl to a final concentration of 1 mg/mL. A 1 mL sample of the (stock) suspension of nonmagnetic (green fluorescent, carboxylated, 39  $\mu\text{m}$ ) microspheres (approximately 400 000 microspheres/mL) was centrifuged at 450 rpm for 1 min. The supernatant was aspirated, and the microspheres were washed with a 0.05% Tween-20 solution (in deionized water). After resuspension of the microspheres, the centrifugation and washing procedure was repeated a second time.

As illustrated in Figure 2 the nonmagnetic microspheres were LbL coated by suspending them in 1 mL of PAH solution; the suspension was continuously vortexed (1000 rpm, 25 °C) for 15 min. The nonadsorbed PAH was removed by repeated centrifugation and washing. Subsequently, the microspheres were dispersed in

(16) Horak, D.; Rittich, B.; Safar, J.; Spanova, A.; Lenfeld, J.; Benes, M. *J. Biotechnol. Prog.* **2001**, 17 (3), 447–452.

(17) Ugelstad, J.; Stenstad, P.; Kilaas, L.; Prestvik, W. S.; Herje, R.; Berge, A.; Hornes, E. *Blood Purif.* **1993**, 11 (6), 349–369.

(18) Aizawa, M.; Burak, J. M. *J. Am. Chem. Soc.* **2006**, 128 (17), 5877–5886.

(19) Minelli, C.; Geissbuehler, I.; Hinderling, C.; Heinzelmann, H.; Vogel, H.; Pugin, R.; Liley, M. *J. Nanosci. Nanotechnol.* **2006**, 6 (6), 1611–1619.

(20) Krishnamoorthy, S.; Hinderling, C.; Heinzelmann, H. *Mater. Today* **2006**, 9 (9), 40–47.

(21) Bhat, R. R.; Fischer, D. A.; Genzer, J. *Langmuir* **2002**, 18 (15), 5640–5643.

(22) Skirtach, A. G.; Déjugnat, C.; Braun, D.; Susha, A. S.; Rogach, A. L.; Sukhorukov, G. B. *J. Phys. Chem. C* **2007**, 111 (2), 555–564.

(23) Decher, G. *Science* **1997**, 277 (5330), 1232–1237.

(24) Caruso, F.; Caruso, R. A.; Mohwald, H. *Science* **1998**, 282 (5391), 1111–1114.

(25) Sukhorukov, G. B.; Donath, E.; Lichtenfeld, H.; Knipfel, E.; Knipfel, M.; Budde, A.; Mohwald, H. *Colloids Surf., A: Physicochem. Eng. Aspects* **1998**, 137 (1–3), 253–266.

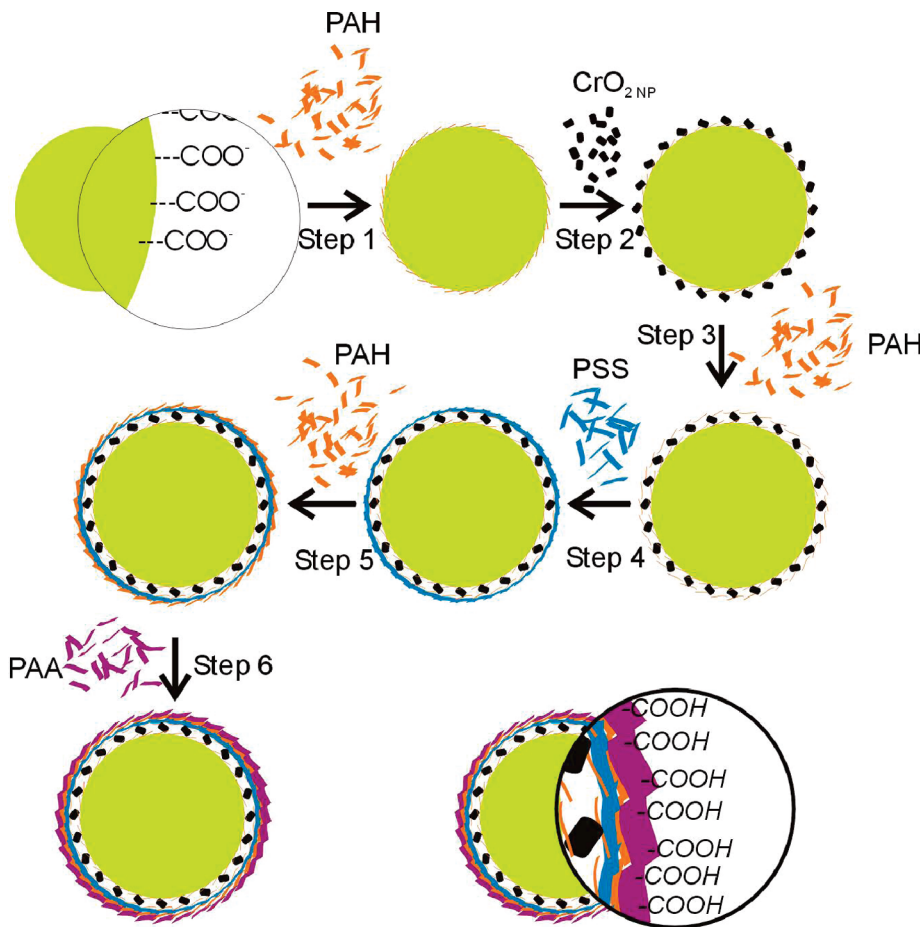


**Figure 2.** Schematic representation of the LbL coating of microspheres. Oppositely charged polyelectrolytes are sequentially adsorbed on the negatively charged nonmagnetic polystyrene microspheres (PAH = poly(allylamine hydrochloride); PSS = poly(styrenesulfonate); PAA = poly(acrylic acid)). Ferromagnetic chromium dioxide nanoparticles ( $\text{CrO}_2$  NPs;  $<450$  nm) are added between two PAH layers.

deionized water containing the sub 500 nm chromium dioxide nanoparticles ( $\text{CrO}_2$  NPs) which were obtained by filtration of a chromium dioxide nanoparticle dispersion through a membrane filter with 450 nm pores. The size of the  $\text{CrO}_2$  NP was measured with a Zetasizer Nano ZS (Malvern, Worcestershire, U.K.). The microsphere dispersion was continuously shaken for 15 min, and the excess  $\text{CrO}_2$  NPs were removed by repeated centrifugation/washing steps. The third, fourth, ... polyelectrolyte layers were applied similarly to the first layer. Finally, the microspheres were coated with six layers in the following order: PAH/ $\text{CrO}_2$  NPs/PAH/PSS/PAH/PAA.

These LbL-coated microspheres were resuspended in 1 mL of deionized water and subsequently encoded (see below).

**Encoding of the Microspheres.** The LbL-coated micropsheres were encoded by spatial selective photobleaching as previously described.<sup>15</sup> An in-house-developed encoding device was used, being a microscopy platform equipped with an Aerotech ALS3600 scanning stage, a SpectraPhysics 2060 argon laser, and an acoustooptic modulator (AA.MQ/A0.5-VIS, A.A-Opto-Electronique, Orsay Cedex, France). The encoding process consists of two steps, a writing step (i.e., the photobleaching process) and a magnetizing step, during which the  $\text{CrO}_2$ -loaded microspheres are exposed to an external magnetic field sufficient to provide them with a magnetic memory. The microspheres are fixed on a grid during the encoding process to avoid rotation of the micropsheres between the two steps.

**Coupling of Oligonucleotides to the LbL-Coated Microspheres.** 5'-Amino-terminal oligonucleotides were covalently attached to the (PAA) carboxyl groups at the surface of the microspheres by one-step carbodiimide chemistry. In brief, approximately 10 000 microspheres were washed three times with 100  $\mu\text{L}$  of 0.4 M MES buffer (0.05% Tween-20, pH 5) and centrifuged. The oligonucleotides were coupled by incubating the micropsheres in 7.5  $\mu\text{L}$  of EDC solution (100 mg/mL in 0.4M MES buffer, immediately used after

preparation) to which 3  $\mu\text{L}$  of oligonucleotides (33  $\mu\text{M}$ ) and 7  $\mu\text{L}$  of MES buffer were added. The reaction was allowed to proceed for 1 h in an Eppendorf thermomixer (at 1500 rpm, 20 °C). Subsequently, the microspheres were washed three times with 100  $\mu\text{L}$  of "assay buffer" (1% BSA, 0.05% Tween-20 in PBS, "blocking step"). They were finally washed another three times with 100  $\mu\text{L}$  of hybridization buffer (5 mM Tris-HCl, 0.5 mM EDTA, 1.0 M NaCl) and stored in 200  $\mu\text{L}$  of hybridization buffer ( $\pm$ 50 000 microspheres/mL) at 4 °C.

**Confocal and Scanning Electron Microscopy Imaging of the Microspheres.** The memobeads were observed using a Bio-Rad MRC 1024 confocal laser scanning system (Bio-Rad, Hemel Hempstead, U.K.) equipped with an inverted microscope (Eclipse TE300D, Nikon, Japan). Images were captured with a Nikon Plan Apochromat 60 $\times$  water immersion objective lens (NA of 1.2, collar rim correction) and with a Nikon Plan Apochromat 10 $\times$  objective lens (NA of 0.45) using the 488 nm laser line from the argon ion laser and the 647 nm laser line from the Ar/Kr laser. For the orientation of the memobeads, a weak external magnetic field was applied with the same orientation as the magnetic field applied during the encoding process (relative to the direction of the laser light). In the presence of this weak magnetic field, the remanent nanoparticles tend to align with the magnetic field, so they will turn the microspheres (at the surface to which they are fixed) into a position that the code can be read (the code is present in a plane perpendicular to the direction of the laser).

The average contrast of the dot code can be defined by the following equation:

$$\text{contrast} = \frac{1}{n} \sum_{i=0}^n \left( \frac{C_{\max,i} - C_{\min,i}}{C_{\max,i}} \right)$$

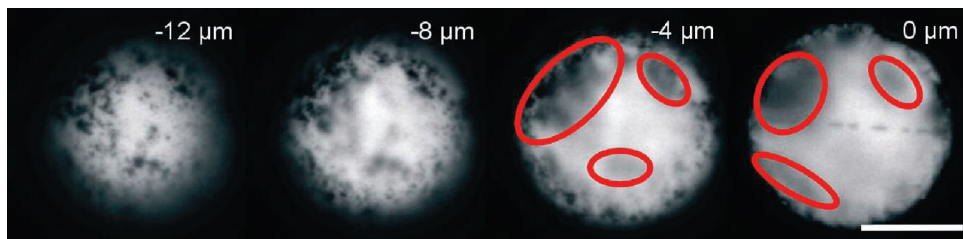
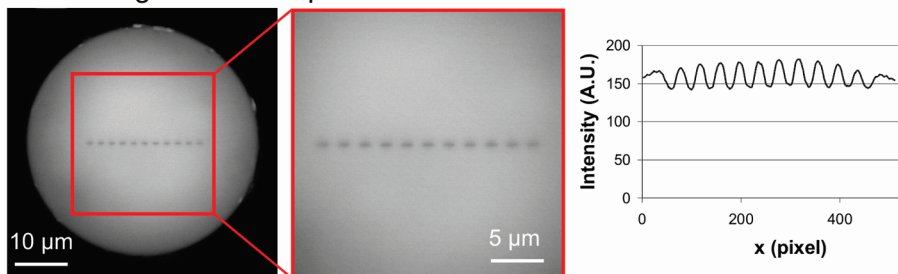


**Figure 3.** Confocal optical sections of a magnetic surface-polymerized encoded microsphere ( $\phi = 39 \mu\text{m}$ ). The dot code is written in the central plane of the microsphere ( $0 \mu\text{m}$ ). Magnetic particles at the surface of the microspheres (leftmost image) result in shaded areas (indicated by the circles), even in the central plane (rightmost image). The scale bar is  $20 \mu\text{m}$ .

A: non-magnetic microsphere



B: magnetic surface-polymerized microsphere

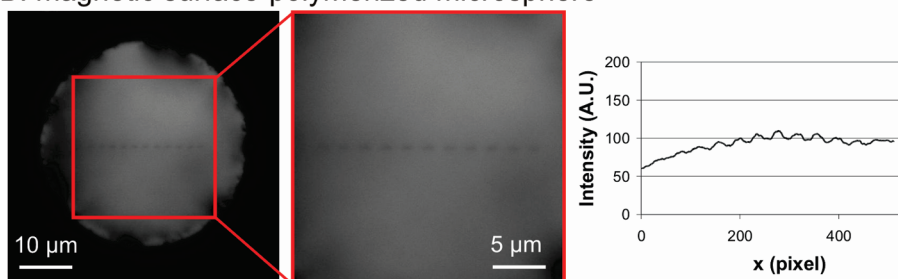


**Figure 4.** Decoding of nonmagnetic (A) and magnetic surface-polymerized (B) microspheres. Left column: confocal images of the central plane of the microspheres. Middle column: magnification of the encoded area. Right column: fluorescence intensity profile measured along the code. In (B), the shadows partially obscure the bleached code segments and do not allow clear visualization of the code. Decoding occurred immediately after the encoding process, thus without any movement/rotation of the microspheres between the encoding and decoding steps.

where  $i$  = a code segment (i.e., a dot),  $n$  = total number of code segments (i.e., number of dots), and  $C$  = fluorescence intensity ( $C_{\max,i}$  and  $C_{\min,i}$  as shown in Figure 7).

The coefficient of variation (CV; %) equals the standard deviation (SD) divided by the average contrast (expressed as a percentage). The standard deviation on the average contrast was calculated as

$$\text{SD} = \sqrt{\frac{\sum_{i=1}^n (x_i - \bar{x})^2}{n-1}}$$

where  $i$  = a code segment (i.e., a dot),  $n$  = total number of code segments (i.e., number of dots), and  $x$  = contrast per segment (i.e., contrast per dot) =  $(C_{\max,i} - C_{\min,i})/C_{\max,i}$ .

To determine the average red fluorescence of one microsphere (due to coupled Cy5-conjugated oligonucleotides), a region of interest (ROI) was drawn around the microsphere and the red fluorescence within the ROI was measured using the Matlab 7.1 version equipped with homemade image processing software. The average red fluorescence of each microsphere was defined as the average of the fluorescence of all pixels within the ROI. The intramicrosphere CV (%) equals the intramicrosphere SD divided by the average red fluorescence (expressed as a percentage). The intramicrosphere

standard deviation on the red fluorescence was calculated as

$$\text{SD} = \sqrt{\frac{\sum_{i=1}^n (x_i - \bar{x})^2}{n-1}}$$

where  $i$  = a pixel within the ROI,  $n$  = number of pixels within the ROI, and  $x$  = fluorescence of a pixel within the ROI.

Scanning electron microscopy (SEM) measurements on memobeads were carried out using a Quanta 200 FEG FEI scanning electron microscope operated at an accelerating voltage of 3 kV. A drop of memobead suspension was deposited onto a silicon wafer and dried under a nitrogen stream followed by sputtering with gold before analysis.

## Results and Discussion

**Ferromagnetic Coating of the Microspheres by Surface Polymerization.** Figure 3 shows confocal images of a ferromagnetic fluorescent polystyrene microsphere which is commercially available. According to the manufacturer's information,

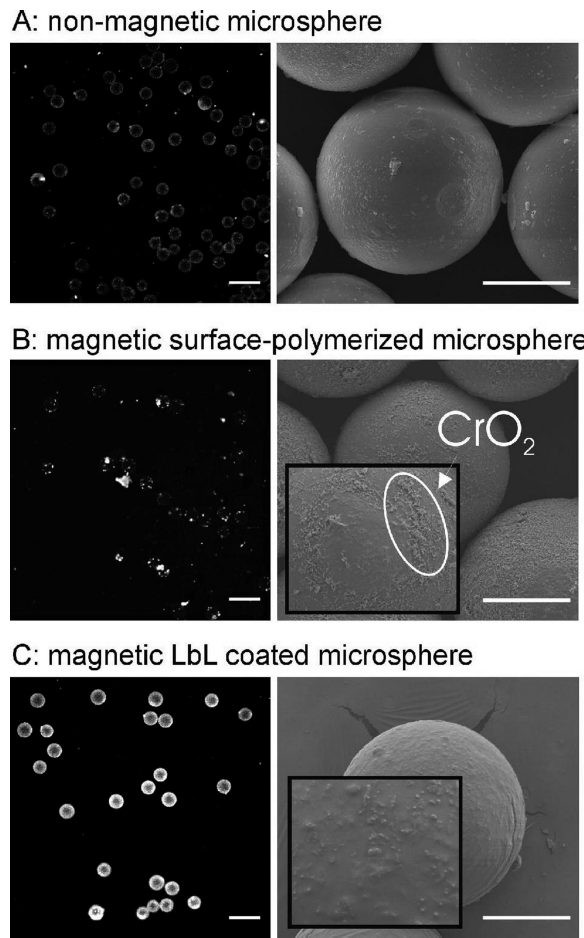


**Figure 5.** Red fluorescence microscopy images (left) and SEM images (right) of nonmagnetic microspheres (A), magnetic surface-polymerized microspheres (B), and magnetic LbL-coated microspheres (C) after the coupling of Cy5-labeled 29-mer oligonucleotides. The scale bar in the fluorescence microscopy images is  $100 \mu\text{m}$ , while it is  $20 \mu\text{m}$  in the SEM images. Even though the laser power to excite Cy5 was approximately 7.5 times less in (A) and (C) (compared to (B)), the red fluorescence at the surfaces of the carriers is less intense in the case of the magnetic surface-polymerized microspheres (B). In (B) aggregated  $\text{CrO}_2$  NPs are heterogeneously spread over the surface and partially present outside the surface. Compared to those in (B), the  $\text{CrO}_2$  NPs at the surface of LbL-coated microspheres (C) do not look so sharp, very likely due to the fact that they are covered with extra polyelectrolyte layers.

the magnetic surface-polymerized microspheres are prepared by entrapping  $\text{CrO}_2$  particles mixed with styrene (monomer) at the surface of premade polystyrene microspheres by polymerization of the styrene. Clearly, the surface of such “surface-polymerized” microspheres is not homogeneously covered with magnetic particles; at certain locations even severe aggregates of  $\text{CrO}_2$  particles can be present. It is important for both encoding and decoding that the microspheres are sufficiently transparent to the laser light and the emitted fluorescence. The chromium dioxide aggregates, however, locally attenuate the laser light and fluorescence. In addition, the chromium dioxide aggregates also cause the appearance of “shadows” in the inner part of the microspheres. Figure 4 shows the result of the decoding of both a nonmagnetic (Figure 4A) and a magnetic (surface-polymerized) (Figure 4B) microsphere carrying a dot code in its central plane. Note that both microspheres were decoded immediately after the encoding process, thus without any movement/rotation of the microspheres between the encoding and decoding steps. The fluorescence intensity is measured along the dot code (right

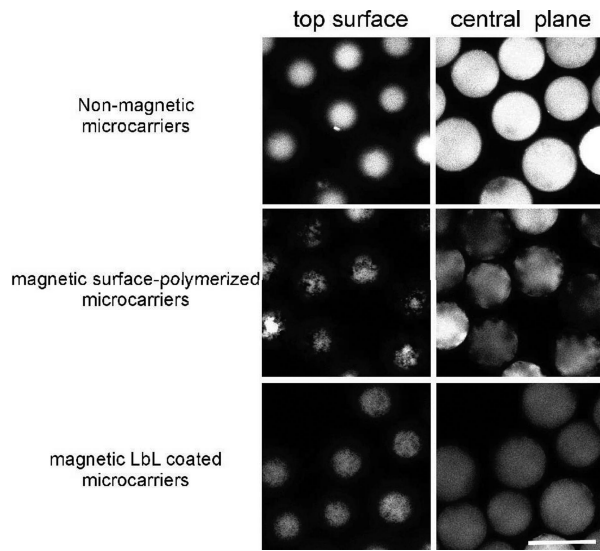


**Figure 6.** Confocal images of the top surface and the central plane of nonmagnetic, magnetic surface-polymerized, and magnetic LbL-coated microspheres. Nonaggregated  $\text{CrO}_2$  NPs are homogeneously distributed over the surface of the magnetic LbL-coated microspheres. Hence, shaded areas are not present in the central plane. The scale bar is  $50 \mu\text{m}$ .

panels). While the dot code can be read perfectly in Figure 4A, in Figure 4B, the shadows partially obscure the bleached code segments and do not allow clear visualization of the code.

Figure 5 shows confocal images of the central plane of both nonmagnetic (Figure 5A, left panel) and magnetic (surface-polymerized) microspheres (Figure 5B, left panel) loaded at their surface with red (Cy5)-labeled 29-mer oligonucleotides. Compared to the surface of the nonmagnetic spheres (Figure 5A), the red fluorescence at the surface of the magnetic (surface-polymerized) microspheres (Figure 5B) seems less homogeneous. This indicates that the surface of the magnetic spheres was not homogeneously covered with the red-labeled 29-mer oligonucleotides. The right panels in Figure 5 show scanning electron microscopy images of the surface of the microspheres. Chromium dioxide particles seem present in the outer surface of the magnetic surface-polymerized microspheres; hence, we expect no polystyrene (and thus no carboxyl groups) at those regions in the surface, which very likely explains why their surface is not homogeneously covered with 29-mer oligonucleotides (Figure 5B, left panel).

**Ferromagnetic Coating of the Microspheres by Layer-by-Layer Technology.** The observations in Figures 4 and 5 clearly show the need to design polystyrene microspheres that (a) are sufficiently magnetic without having chromium dioxide aggregates at their surface (to avoid shadows) and (b) can be homogeneously loaded with capture probes. Therefore, as schematically shown in Figure 2, six layers of polyelectrolytes and ferromagnetic chromium dioxide nanoparticles were applied by LbL technology on the surface of the polystyrene microspheres.<sup>25</sup>  $\text{CrO}_2$  NPs smaller than  $0.45 \mu\text{m}$  (as obtained by the filtration of a chromium dioxide nanoparticle dispersion through a  $0.45 \mu\text{m}$  pore filter) were added between two PAH layers; to obtain carboxyl groups at the surface, the final layer in the LbL coating was PAA.

As the confocal microscopy images of the top surface of the microspheres (Figure 6, left panels) show, when applied by LbL coating the  $\text{CrO}_2$  NPs seem more homogeneously distributed over the surface of the microspheres, without the occurrence of aggregates. This was confirmed by SEM images (see Figure 5C, right panel). Especially, shadows in the central plane of the LbL-

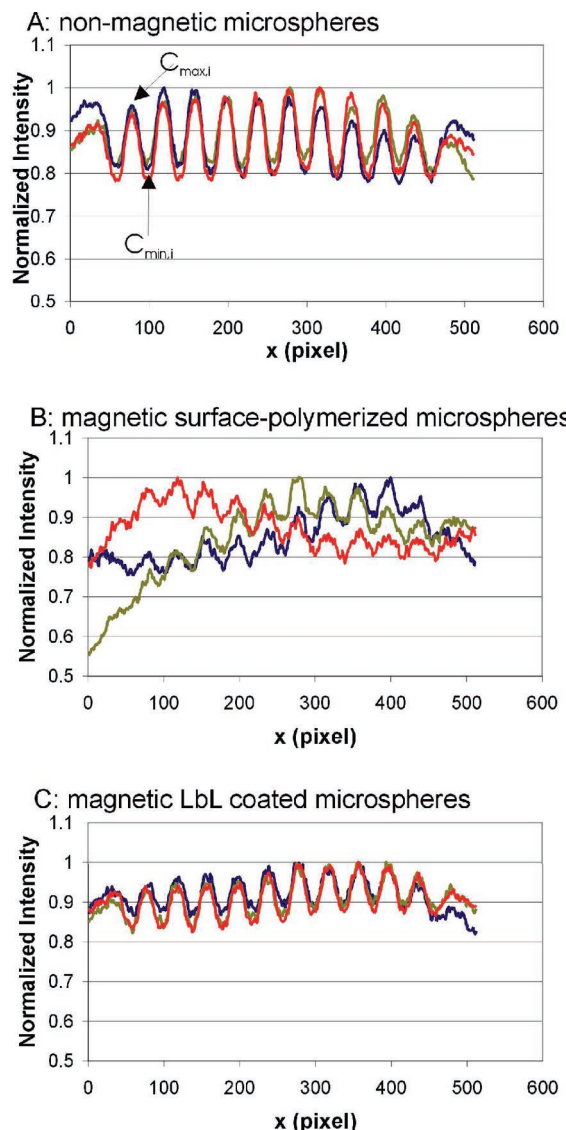


**Figure 7.** Normalized fluorescence intensity profiles of identical dot codes written in the central plane of nonmagnetic microspheres (A; three spheres were encoded), magnetic surface-polymerized microspheres (B; three spheres were encoded), and magnetic LbL-coated microspheres (C; three spheres were encoded). Normalized values were calculated as the ratio between the fluorescence intensity and the maximum fluorescence intensity along the dot code. Decoding occurred immediately after the encoding process, thus without any movement/rotation of the microspheres between the encoding and decoding steps.

coated microspheres were not observed (Figure 6, right panels), which facilitates a correct decoding. Figure 7 shows the (normalized) fluorescence intensity profiles of a dot code written in nonmagnetic, magnetic surface-polymerized, and magnetic LbL-coated microspheres. Note that all microspheres were decoded immediately after the encoding process, thus without

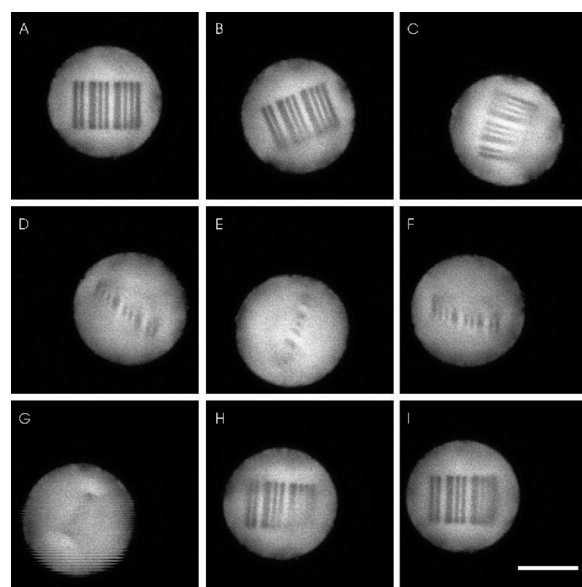


**Figure 8.** A magnetic LbL coating of the microspheres allows bringing the microspheres into a correct readout position. (A) Confocal image of the central plane of a magnetic LbL-coated microsphere just after being encoded with a bar code; during the encoding process the microspheres were exposed to a strong magnetic field to provide them with a remanent magnetic direction. (B–H) Confocal images of the central plane of the microsphere while randomly moving. (I) Confocal image of the central plane of the microsphere upon bringing the microsphere back into a (weak) magnetic field: it turns to its original orientation (compare images A and I), which permits reading of the code. The scale bar is 20  $\mu$ m.

any movement/rotation of the microspheres between the encoding and decoding steps. Clearly, the dot code written in magnetic LbL-coated microspheres (Figure 7C) is much more uniform compared to the dot code written in magnetic surface-polymerized microspheres (Figure 7B). This observation is supported quantitatively by the information in Table 1.

The average contrast for the different kinds of beads is reported together with the corresponding coefficient of variation. We have also added the “normalized minimum”, which is the lowest contrast value found in the dot code. The profiles of the codes written in the central plane of the surface-polymerized microspheres exhibit a very high CV (37% on average), compared to that of nonmagnetic microspheres (15% on average), due to the presence of code segments that are almost indistinguishable from the unbleached background fluorescence (which can also be seen in Table 1 from the normalized minimum values). The CVs along the dot code profiles measured in the magnetic LbL-coated microspheres, however, are 12% on average, which is far below that of the magnetic surface-polymerized microspheres and similar to that of the nonmagnetic microspheres. Here all code segments are clearly distinguishable from the unbleached local background fluorescence, as can be seen in Table 1 from the normalized minimum values.

**Table 1. Contrast Values (and Corresponding CVs) Measured along the Dot Code Intensity Profiles of Figure 7<sup>a</sup>**

	nonmagnetic microspheres		magnetic surface-polymerized microspheres		magnetic LbL-coated microspheres	
	contrast	CV (%)	contrast	CV (%)	contrast	CV (%)
0.153	18	0.112	0.079	27	0.051	0.083
0.141	16	0.100	0.068	46	0.005	0.094
0.171	12	0.133	0.066	38	0.017	0.105

<sup>a</sup> Normalized minimum = code segment which minimally differs from the unbleached local background fluorescence =  $[(C_{\max,i} - C_{\min,i})/C_{\max,i}]_{\min}$ .

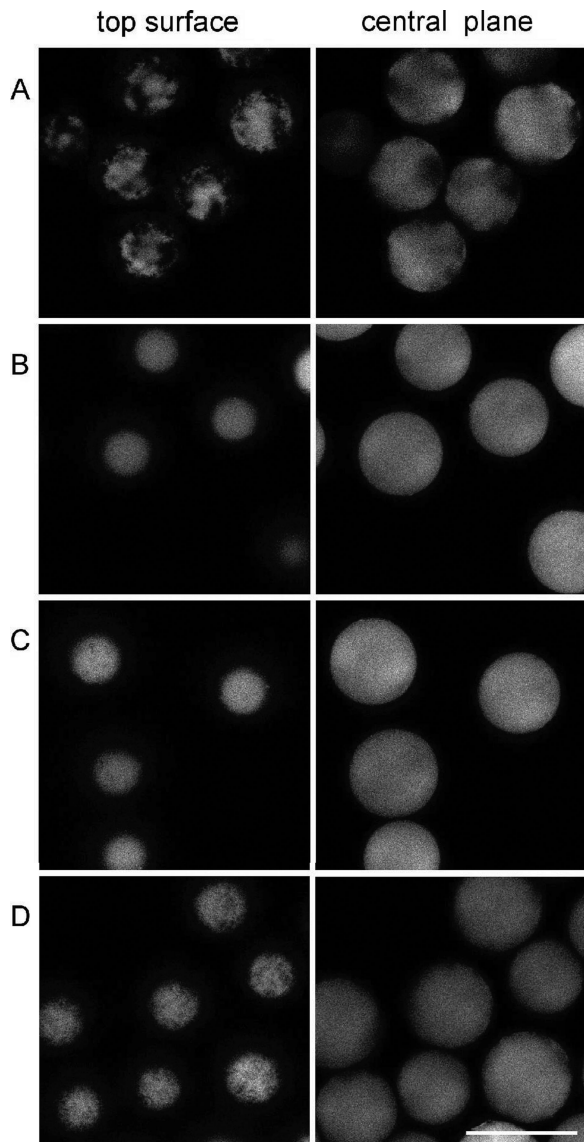


**Figure 9.** Confocal images of the top surface and the central plane of magnetic surface-polymerized microspheres (A) and magnetic LbL-coated microspheres (B–D). The latter ones were coated with  $\text{CrO}_2$  NPs with different sizes (B,  $< 100$  nm; C,  $< 220$  nm; D,  $< 450$  nm). The smaller the  $\text{CrO}_2$  NPs, the fewer the shadows at the central plane. However, when the microspheres were coated with  $\text{CrO}_2$  NPs smaller than 220 nm, their positioning did not always work perfectly. The scale bar is 50  $\mu\text{m}$ .

Note that, in this paper, 39  $\mu\text{m}$  sized polystyrene microspheres are used. The LbL coating procedure can be applied on microspheres with other sizes as well. The minimal size of the microspheres is especially determined by the length of the code which has to be written in the microspheres. For more information regarding the length of the code, we refer to Braeckmans et al.<sup>15</sup>

**Positioning of Magnetic LbL-Coated Microspheres in a Magnetic Field.** Figure 8 shows a magnetic LbL-coated barcode polystyrene microsphere exposed to a magnetic field: the  $\text{CrO}_2$  NPs in the LbL coating and the magnetic field bring the bar code to the position allowing readout of the code. We note that the  $\text{CrO}_2$  NPs (a) keep their magnetic memory, as expected, and (b) are immobilized in the LbL coating, which is also a requirement to be able to properly orient the microspheres upon application of the magnetic field for decoding. The fact that the  $\text{CrO}_2$  NPs are sufficiently fixed on the microspheres is not sur-

**Table 2. Analysis of the Coupling of Cy5-Labeled 29-Mer Oligonucleotides to the Carboxyl Groups at the Surface of Eight Nonmagnetic Microspheres, Eight Surface-Polymerized Microspheres and Eight LbL-Coated Microspheres<sup>a</sup>**

nonmagnetic microspheres		magnetic surface-polymerized microspheres		magnetic LbL-coated microspheres	
average fluorescence	CV (%)	average fluorescence <sup>b</sup>	CV (%)	average fluorescence	CV (%)
40.5	39.3	39.0	80.1	179.3	37.4
49.3	39.9	24.4	65.1	130.7	42.9
47.4	37.7	27.0	84.3	172.3	37.5
42.6	38.0	22.3	68.6	176.3	38.3
56.1	36.1	27.1	60.8	167.2	41.1
40.0	33.0	38.2	96.6	138.4	47.8
40.8	39.1	26.3	90.5	118.4	40.8
41.0	31.4	20.1	81.6	175.6	47.5

<sup>a</sup> Although the power of the laser to excite Cy5 was approximately 7.5 times less in the case of the nonmagnetic and the magnetic LbL-coated microspheres (compared to the magnetic surface-polymerized microspheres), the red fluorescence at the surface is less intense in the case of the magnetic surface-polymerized microspheres. <sup>b</sup> Higher excitation (7.5 times).

prising since they are strongly bound by electrostatic interactions with the polycations of the LbL coating (Figure 2).

On one hand, smaller  $\text{CrO}_2$  NPs allow a more uniform readout of the code because the shadows in the central plane are less pronounced. On the other hand, the force required to turn the microspheres into the appropriate position, which is related to the size and amount of the magnetic  $\text{CrO}_2$  NPs, should be strong enough to overcome the interaction forces between the microsphere and the glass surface of the recipient. Figure 9 shows polystyrene microspheres that were LbL coated with  $\text{CrO}_2$  NPs differing in size ( $< 100$ ,  $< 220$ , and  $< 450$  nm). The  $\text{CrO}_2$  NPs were obtained by filtration of a chromium dioxide nanoparticle dispersion through respectively 100, 220, and 450 nm pore filters. When the microspheres were coated with  $\text{CrO}_2$  NPs smaller than 220 nm, their positioning, upon application of a magnetic field, did not always work perfectly. This means that the total magnetic force of the sub 220 nm sized nanoparticles, coated on one microparticle, was not high enough to turn the relatively huge microparticle, conversely to the positioning of microspheres coated with larger  $\text{CrO}_2$  NPs, which occurred immediately upon application of the magnetic field. We concluded that the preferred size range of the  $\text{CrO}_2$  NPs is between 220 and 450 nm.

**Capturing Oligonucleotides at the Surface of LbL-Coated Encoded Microspheres.** Parts B and C of Figure 5 (left panels) show fluorescence images of both magnetic surface-polymerized and magnetic LbL-coated microspheres loaded at their surfaces with Cy5-labeled 29-mer oligonucleotides. Unlike the surfaces of surface-polymerized microspheres, the surfaces of the LbL-coated ones seem more homogeneously covered with Cy5-labeled oligonucleotides. This is most likely due to the fact that the  $\text{CrO}_2$  NPs at the surface of the microspheres were also coated with PAA (Figure 2), providing the whole surface of the beads with carboxyl groups. From the SEM images in Figure 5 one can clearly see that the  $\text{CrO}_2$  NPs are coated with extra polymer layers: the particles do not look as sharp (5C, right panel) as when they are not covered (5B, right panel). This is also confirmed in Table 2, where the red fluorescence intensity values at the surfaces of nonmagnetic, magnetic surface-polymerized, and magnetic LbL-coated microspheres is analyzed. The magnetic LbL-coated microspheres have an *intramicrosphere* CV on their red fluorescent signal of around 40%, which is similar to that of the nonmagnetic microspheres. The magnetic surface-

polymerized ones, however, show CVs of approximately 70–90%, indicating that the probes are inhomogeneously loaded across the surface. The magnetic LbL-coated microspheres also have an increased loading capacity, as can be seen from the average red fluorescence, which is 4 times higher than that of the nonmagnetic ones. While the nonmagnetic and LbL-coated microspheres have similar *intermicrosphere* CVs (respectively 14.2% and 13.8%), the magnetic surface-polymerized microspheres show a higher *intermicrosphere* CV of around 27%. In addition, the average red fluorescence of the latter ones is approximately 50 times less than that of the magnetic LbL-coated microspheres. Clearly, besides the improved visibility of the code, the LbL coating of the microspheres also increases the capacity (and quality) to load probes (such as oligonucleotides) at the surface, which can be easily explained by the fact that LbL coating results in a higher number of carboxyl groups at the surface.

### Summary and Conclusions

A “multifunctional” layer-by-layer coating, containing CrO<sub>2</sub> NPs, was applied at the surface of digitally encoded microspheres. We showed that the LbL coating allows (a) an optimal (optical) readout of the codes, (b) a perfect orientation (within pixel

accuracy (0.7 μm/pixel) of the microspheres (leading to a correct decoding), and (c) an optimal coupling of capture probes to the surface. Thus far, the potential of LbL coating has been explored in a number of applied scientific fields such as drug delivery,<sup>26–28</sup> for corrosion protection,<sup>29</sup> and for the production of biosensors.<sup>30</sup> To our knowledge this is one of the first studies that experimentally demonstrate that LbL technology indeed allows the application of coatings with various advanced functionalities. We are currently investigating whether the LbL coatings surrounding the microspheres would also allow us to quantitatively measure analytes (such as proteins and nucleic acids) in biological samples such as serum and blood.

LA701059Z

- 
- (26) Ai, H.; Jones, S. A.; Lvov, Y. M. *Cell Biochem. Biophys.* **2003**, *39* (1), 23–43.
- (27) Wood, K. C.; Boedicker, J. Q.; Lynn, D. M.; Hammon, P. T. *Langmuir* **2005**, *21* (4), 1603–1609.
- (28) De Geest, B. G.; Dejugnat, C.; Sukhorukov, G. B.; Braeckmans, K.; De Smedt, S. C.; Demeester, J. *Adv. Mater.* **2005**, *17* (19), 2357.
- (29) Shchukin, D. G.; Zheludkevich, M.; Yasakau, K.; Lamaka, S.; Ferreira, M. G. S.; Mohwald, H. *Adv. Mater.* **2006**, *18* (13), 1672.
- (30) Ferreira, M.; Fiorito, P. A.; Oliveira, O. N., Jr.; Cordoba de Torresi, S. I. *Biosens. Bioelectron.* **2004**, *19* (12), 1611–1615.